Bull. Mater. Sci., Vol. 39, No. 1, February 2016, pp. 69–77. © Indian Academy of Sciences.

# Size-controlled synthesis of biodegradable nanocarriers for targeted and controlled cancer drug delivery using salting out cation

**MADASAMY HARI BALAKRISHANAN and MARIAPPAN RAJAN***
Department of Natural Products Chemistry, School of Chemistry, Madurai Kamaraj University, Madurai 625 021, India

MS received 23 January 2015; accepted 16 February 2015

**Abstract.** **Research for synthesis of size-controlled carriers is currently challenging one. In this research paper, a method for size-controlled synthesis of biodegradable nanocarriers is proposed and described. Salting out method is suitable for both hydrophilic and hydrophobic drugs for the encapsulation on carriers. This synthetic method is based on polylactic acid (PLA) and non-ionic carboxymethyl cellulose (CMC) composed by $CaCl_2$ as salting out agent. This method permits size-controlled synthesis of particles between 50 and 400 nm simply by varying the concentration of salting out agents. We have prepared cisplatin (CDDP)-loaded PLA-CMC nanocarriers by salting out method, with varying salting out agent ($CaCl_2$) concentrations as 0.05, 0.2, 0.35 and 0.5 M. The nanocarriers were characterized for their size, surface charge and morphology by atomic force microscope, zeta potential analyser and transmission electron microscope, respectively. The encapsulation efficiency and *in-vitro* drug-releasing behaviour of the nanocarriers were investigated. The cytotoxicity effect of nanocarriers and drug-loaded nanocarriers was tested against MCF-7 breast cancer cell line.**

**Keywords.** **Biodegradable; carboxymethyl cellulose; polylactic acid; size controlled; salting out.**

## 1. Introduction

Multidisciplinary scientific field is undergoing explosive advancement in nanotechnology for the manufacturing of systems or device at the molecular level [1]. Nanotechnology is ultimately used to design drug-loaded carriers, and products of various field with new enhanced properties, new components, new types of 'smart' medicines, sensors and particularly in the field of medicine is delightful in monitoring, diagnosing, preventing, repairing or curing diseases and damaged tissues in biological systems [2]. Design of molecular self-assembly at the nano level is an innovative and promising direction for nanomedicine, as many physiological and pathological processes require interactions between biomolecular building blocks to form ordered nanoassemblies. Nanoparticles for cancer chemotherapeutics area is quickly evolving and produced an enrichment of outcomes. The results of the outcomes have beat many limitations of typical small-molecule chemotherapeutics [3]. Design and synthesis of carriers within the nanoscale provide the benefits of increased delivery efficiency, targeting, controlled releases and talent to bypass biological barriers [4,5]. Nanoparticles have comparatively higher intracellular uptake compared to microparticles ($>1$ μm), because particle size comprises a vital impact on their circulation time and targeting delivery [6,7]. In particularly, the effective delivery of the drug in the epithelium of the blood vessels in numerous human tumours has been according to the pore size, which varies from 200 to 600 nm. Therefore, there is an accord that particles should be less than 200 nm and ideally but a 100 nm to learn from the enhanced porosity and retention [8]. The uptake of drug on cell is highly challenging to delivery especially targeted delivery. Interactions of nanoparticles with components of the outer surface of cells and cellular membranes were followed by internalization into vesicles. The endocytic pathway depends on the size, morphology and surface chemistry of the nanoparticles and varies from one cell line to another [9].

Currently it is a challenge to design drug-loaded carriers with the smaller size than those mentioned size measurable relation. There are many methods available for the preparation of drug-loaded nanocarriers. Among these, solvent evaporation technique, double emulsion technique, solvent displacement/precipitation technique, emulsification–diffusion technique, spray drying technique and salting out technique are the foremost common methods [10–13]. The choice of acceptable technique for the preparation of nanoparticles depends on the chemistry character of the polymeric carriers and also the drug to be loaded. In solvent evaporation technique and double emulsion techniques, water incompatible organic solvents were used and then these methods were not appropriate for hydrophilic drug and additionally unsafe organic solvent usage can cause build, as it is unsuitable for clinical purpose [14]. Other methods such as solvent displacement technique [15], solvent diffusion technique [16] and spray drying method [17] were also handled with harmful organic solvent and with the appurtenant instrumentation it is incredibly high-priced and additionally the thermal potency is incredibly low. Salting out technique has several

*Author for correspondence (rajanm153@gmail.com)

benefits over the other methods, such as low energy consumption, speedy method and want of less unsafe organic solvent etc [10]. Salting out technique is a modified version of emulsion process that involves a salting out process, which avoids toxic organic solvents. In salting out method, electrolyte was used for the separation of organic solvent. Commonly magnesium chloride, calcium chloride and magnesium acetate are used as suitable electrolyte [18].

In this study, calcium chloride was used as salting out agent because calcium chloride is easily dissociated into calcium and chloride ions in water. The absorption, distribution and excretion of the ions in animals are regulated separately. Both ions in certain level are essential constituents of the body of all animals. Calcium is essential for the formation of skeletons, neural transmission, muscle contraction, coagulation of the blood and so on. From the Hoffmeister series $Ca^{2+}$ has high ability to induce selective precipitation on many interactions with the water and solutes. In this study, we controlled the size of polylactic acid (PLA) crosslinked with carboxymethyl cellulose (CMC) using various concentrations of $CaCl_2$ (salting out agent). PLA is a biodegradable polymeric material with low toxicity, excellent biocompatibility and bioabsorbability *in vivo* [19]. In the body, PLA is hydrolysed and decomposed to their monomeric components, lactic acid also occurs physiologically as by-products of several metabolic pathways, and there is no systemic toxicity associated with their use as nanoparticulate drug delivery systems [20]. CMC as a natural polymer has great potential for providing a broad range of important functional properties and possesses several advantages that make them excellent materials for industrial and biomedical use; they are nontoxic, renewable, biodegradable and modifiable [21].

## 2. Materials and methods

### 2.1 *Materials*

PLA, CMC and acetic acid were obtained from Merck Chemical Company Inc. (Mumbai, India). Calcium chloride, acetone, dimethyl sulphoxide (DMSO) and phosphate buffer saline (PBS) were purchased from Himedia Chemical Company Inc. (Mumbai, India). Cisplatin drug and 3-(4,5-dimethylthiazol-2-yl)-2,5-diphenyltetrazolium bromide (MTT) reagent were purchased from Sigma, India. MCF-7 cell line was obtained from American Tissue Cell Culture, USA. All of these chemicals were used as analytical grade and all solutions were prepared using triply distilled water.

### 2.2 *Preparation of nanoparticles*

Nanoparticles were prepared by following salting out method reported by Galindo-Rodriguez *et al* [22] with slight modification. Briefly, CMC is dissolved in 20 ml of 0.05 M $CaCl_2$ solution in a beaker under mechanical stirring. In another vessel, PLA and CDDP drug are dissolved in 10 ml acetone. This acetone part is suddenly poured into the aqueous part. This system is allowed to stir for about 3 h under mechanical stirring at 1500 rpm. Some amount of water is added to the system. Then the formed nanoparticles are collected by high-speed centrifuge (3000 rpm for 10 min; REMI-800). This same procedure is followed for 0.2, 0.35 and 0.5 M $CaCl_2$ solution as aqueous phase and for the preparation of drug unloaded nanocarriers.

### 2.3 *Characterization of nanoparticles*

2.3a *FT-IR spectral analysis*: The FT-IR spectra of the samples were recorded using a Fourier transform infrared spectrometer (FT-IR; Spectrum GX-1, PerkinElmer, USA). Briefly, a small quantity of the nanoparticles was mixed with 200 mg of KBr and compressed to form tablets. These tablets were scanned in transmission mode in the spectral region of 4000–400 $cm^{-1}$ using a resolution of 4 $cm^{-1}$ and 32 co-added scans.

2.3b *Atomic force microscopy analysis*: Atomic force microscope (AFM) images were obtained using a Multimode Scanning probe microscope (NTMDT, NTEGRA prima, Russia) in non-contact mode with a PPP-NCHR cantilever with a 330 kHz resonant frequency. The scan speed was between 0.5 and 1.5 Hz using the adaptive scan mode function set in the software. All of the images contained 256 × 256 data points. For AFM visualization, a drop of the diluted nanoparticle suspension (0.1 mg $ml^{-1}$) was drop casted onto a flat microscopy glass. After overnight evaporation, the sample was processed directly on the AFM scanner. To obtain high-resolution images of the nanoparticles deposited onto the substrate, PPP-NCHR silicon cantilevers with a length of 125 μm were typically used with a resonant frequency of approximately 270 kHz and a nominal force constant near 42 N $m^{-1}$. A constant tip-to-sample distance was maintained using the amplitude feedback function in the attractive forces regimen to prevent damage to the nanoparticles.

2.3c *Transmission electron microscope analysis*: The morphology of the nanoparticles was observed using transmission electron microscope (TEM). The TEM images of the nano particles were acquired by Technai G2–TF 20 (FEI) microscope, which was operated at 200 kV. Films with a width of 1 mm were placed in Eppendorf tubes and gradually infiltrated at 24°C using a Spurr resin/ethanol gradient (30% resin for 8 h, 70% resin for 12 h and three cycles of 100% resin for 24 h each). After infiltration, the films were mounted in the mould and cured in an oven at 65°C for 24 h.

2.3d *Zeta potential of blank and drug-loaded nanoparticles*: For the measurement of surface charge potential value of the nanoparticles, accurately weighed 10 mg of nanoparticles was suspended in 10 ml deionized water before the experiments and Beckman culter (DelsaTM Nano; Malvern

Instruments Ltd, UK) was used in this study. The data obtained were the average of three measurements.

### 2.4 *Evaluation of encapsulation efficiency*

The nanoparticle suspensions were separated by centrifugation at 2500 rpm for every 30 min and the drug encapsulation efficiency (EE) of the nanoparticles were evaluated by measuring the absorption of the supernatant using a UV spectrophotometer (Systronics, India). The corresponding calibration curves were calculated by testing supernatant of blank solution. The absorption of free CDDP present in the supernatant solution was measured at the λ-max value of 265 nm. All the measurements were performed in triplicate and mean values were reported.

### 2.5 *In-vitro drug release measurement*

The *in-vitro* experiment of CDDP release from various encapsulated carriers was performed by following the procedure reported by Tabatabaei Rezaei *et al* [23]. In brief, the nanoparticles weighed accurately (100 mg) and immersed with 5 ml pH (pH 2.0/6.8) solution in the dialysis bag (MWCO 3 kD) allowed the small molecules to pass through while holding back the macromolecules (molecular weight >3000 kD). A volume of 95 ml of pH solution (pH 2.0/6.8) was added into the 250 ml beaker with stirring and the immersing temperature was kept at room temperature. The dialysis bag was put into slow release system. At a given time (30 min), the solution (3 ml) was removed for measurement of free CDDP into the solution and an equal volume of fresh PBS solution was immediately added to keep the volume constant. The content of the CDDP in each aliquot was measured by the absorbance at 265 nm by using a UV spectrophotometer (Systronics, India).

### 2.6 *Cytotoxicity effect of nanoparticles*

The cytotoxicity effect of the nanoparticles was tested by MTT viability assay against MCF-7 breast cancer cell line. MCF-7 breast cancer cells were seeded in 96-well plates ($5 \times 10^3$ cells per well) in 100 ml of minimum essential medium supplemented with 10% fetal bovine serum, 1% penicillin/streptomycin and 0.15% insulin (10 mg $ml^{-1}$) at 37°C under a humidifying atmosphere containing 5% $CO_2$. After 24 h of incubation to allow cell adhesion, the 22 medium in each well was replaced with 150 ml of new

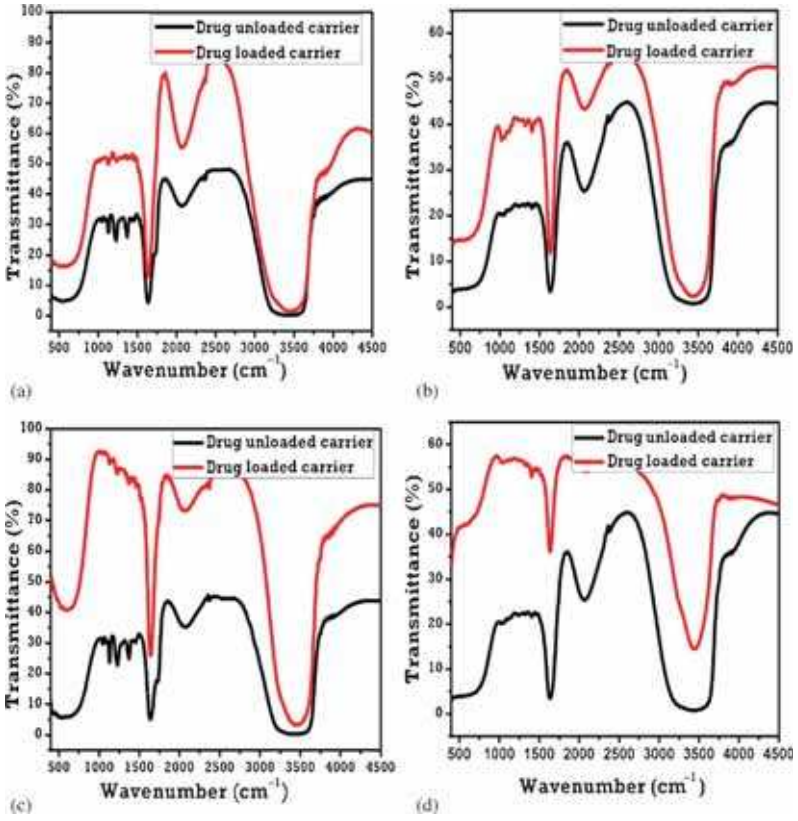


**Figure 1.** FT-IR spectrum of (**a**) PLA-$CaCl_2$-CMC-A, (**b**) PLA-$CaCl_2$-CMC-B, (**c**) PLA-$CaCl_2$-CMC-C and (**d**) PLA-$CaCl_2$-CMC-D carriers with and without CDDP.

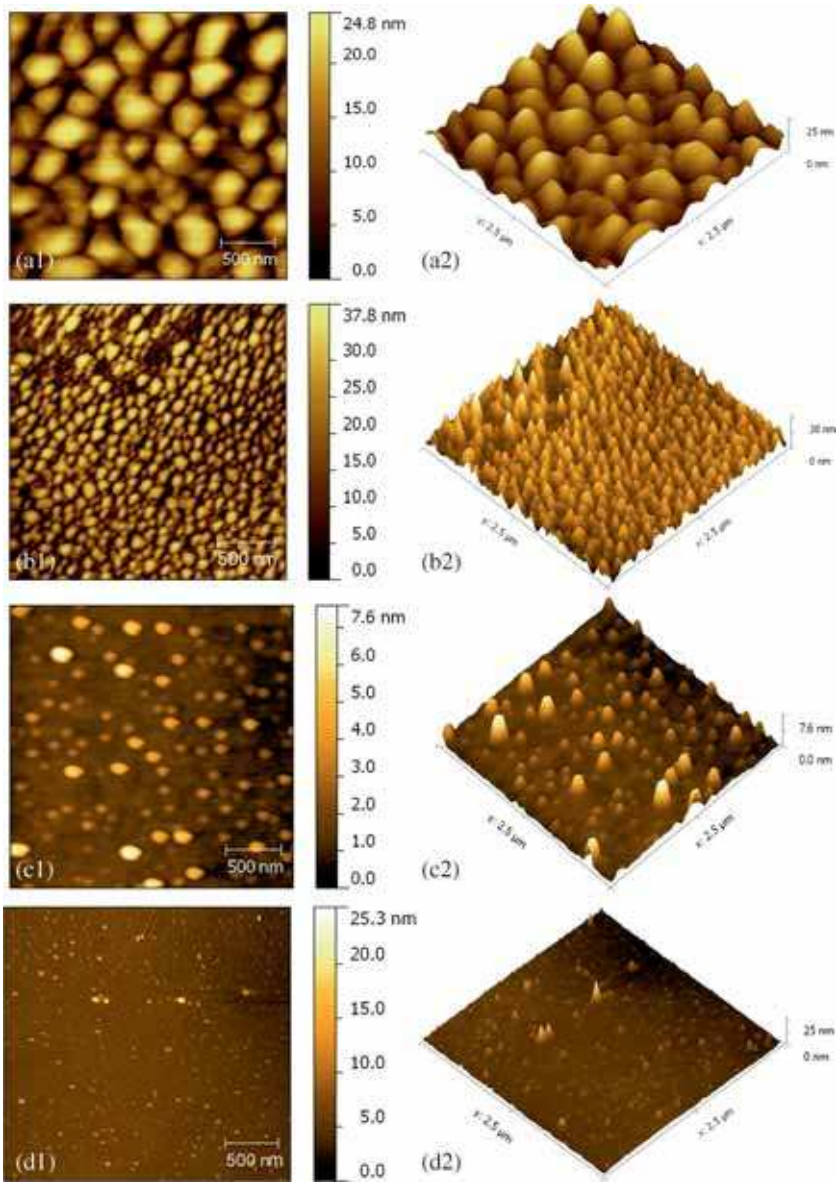


**Figure 2.** AFM image of (**a**) PLA-$CaCl_2$-CDDP-CMC-A, (**b**) PLA-$CaCl_2$-CDDP-CMC-B, (**c**) PLA-$CaCl_2$-CDDP-CMC-C and (**d**) PLA-$CaCl_2$-CDDP-CMC-D nanocomposites.

medium containing the serial dilution of CDDP, PLA-$CaCl_2$-CMC-A, PLA-$CaCl_2$-CMC-CDDP-A, PLA-$CaCl_2$-CMC-B, PLA-$CaCl_2$-CMC-CDDP-B, PLA-$CaCl_2$-CMC-C, PLA-$CaCl_2$-CMC-CDDP-C, PLA-$CaCl_2$-CMC-D and PLA-$CaCl_2$-CMC-CDDP-D nanocomposites at various concentrations (10–100 μM), and cells were then incubated at 37°C in 5% $CO_2$ for 24 h. After incubation for each time period, the medium in each well containing all the samples were aspirated and the cells were washed with PBS. For cell viability measurements, 100 ml of fresh medium (free of phenol red) and 10 ml of MTT reagent (5 mg $ml^{-1}$ in PBS) was added to each well and incubated for 4 h to allow the formation of formazan crystals. After removing all, but 25 ml, the medium from the wells, 50 ml of DMSO was added to each well (to solubilize the formazan) mixed thoroughly and incubated at 37°C for an additional 10 min. The absorbance values were measured using a microplate reader (Bio-Rad, model 680) at 570 nm to determine relative viabilities. Data are presented as average ± SD.

### 2.7 *Statistical analysis*

Mean comparisons were made by analysis of variance and protected least significant difference. Contrasts were considered significant at $P < 0.05$. Data were reported as means ± standard errors.

## 3. Results and Discussion

### 3.1 *Preparation of nanoparticles*

Cisplatin-loaded PLA–CMC nanoparticles were successfully prepared by following the salting out method, which

was reported by Galindo-Rodriguez *et al* [22]. Salting out is based on the separation of a water miscible solvent from aqueous solution via salting out effect [24]. Here high concentration of calcium chloride will prevent the miscibility of acetone part into the aqueous medium. On mechanical agitation of this system, emulsion of acetone in water is formed. The formed emulsion droplet size will be controlled by the concentration of salting out agent. On dilution of this system with sufficient amount of water leads to the diffusion of acetone part into the aqueous medium. Due to this action cisplatin-loaded polymer nanocarrier gets precipitated. The increasing concentration of salting out agent reduced the size of particles.

### 3.2 *Characterizations of the nanoparticles*

3.2a *FT-IR spectroscopy*: Functionalization of the nanocarriers was characterized by using FT-IR spectroscopy. The FT-IR spectra of CDDP drug loaded and unloaded of four pairs of polymeric nanocarriers are shown in figure 1. The resulting absorption at 1620 $cm^{-1}$ is due to the –COO group of PLA and CMC present in carriers [25]. The absorption peak appearing at 3480 $cm^{-1}$ was corresponding to –OH group present in PLA and CMC [26]. The broadening of –OH peak was due to intermolecular hydrogen bonding between hydroxyl group hydrogen atom and the oxygen atom present in PLA and CMC [25,28]. The other bands present at the range of 1110–1500 $cm^{-1}$ was due to the overlapping signals of C–O stretching and O–H bending [27,29]. C–H stretching frequency absorption band at 1453 $cm^{-1}$ and C–H deformation vibration at 1362 $cm^{-1}$ was with respect to methyl group present in PLA [30]. In the drug-loaded nanoparticle spectrum, an additional absorption occurs at 3236 $cm^{-1}$. This absorption is due to the N–H stretching of $NH_3$ group present in cisplatin molecule, which was encapsulated by nanocarriers [31]. This particular characteristic peak was not present in the drug unloaded nanoparticle. The broadness of the peak is due to the intermolecular hydrogen bonding between the cisplatin and carrier. However in the case of 0.5 M $CaCl_2$ crosslinked polymer carrier, the intermolecular hydrogen bonding is missed. This may be due to the excess of $Ca^{+2}$ ions that lead to form coordinate covalent bond with the carrier, which leads to the separation of the nanoparticles. It is well correlated to EE and *in-vitro* drug release properties of carriers.

3.2b *AFM analysis*: The surface topography of nanocomposites was measured by AFM. The AFM images of CDDP-loaded polymeric nanocarriers PLA-$CaCl_2$-CDDP-CMC-A, PLA-$CaCl_2$-CDDP-CMC-B, PLA-$CaCl_2$-CDDP-CMC-C and PLA-$CaCl_2$-CDDP-CMC-D are shown in figure 2. By utilizing sensitive morphological technique of AFM, we were able to obtain highly detailed images of polymeric nanoparticles. The 3D AFM image of nanoparticles clearly indicated the size and structural morphology of particles that changed with increasing concentration of $CaCl_2$. The size distribution was obtained by applying the Watershed algorithm with filter level 1 to a 2.5 × 2.5 μm image; under this condition, PLA-$CaCl_2$-CDDP-CMC-A gave information that the particles are in the range from 50 to 400 nm, PLA-$CaCl_2$-CDDP-CMC-B showed that the particles range from 60 to 350 nm, PLA-$CaCl_2$-CDDP-CMC-C result was from 70 to 300 nm and PLA-$CaCl_2$-CDDP-CMC-D image indicates that its size ranges from 80 to 200 nm. The RMS value of four images was 150, 140, 130 and 120 nm, respectively. The size of the nanoparticle was changed with decreasing or increasing concentration of $CaCl_2$. This fact arises due to the increasing nature of immiscibility of acetone in high concentrate calcium chloride solution, so the emulsion droplet formed should have very small size in nature. Definitely, AFM measurements are in good agreement with nanoparticles on glass to keep intact their spherical morphology and dimension.

3.2c *Surface morphology and charge of the nanoparticles*: Interestingly, drug-loaded nanocarriers resulted in smaller particle sizes while maintaining $CaCl_2$ concentration from 0.05 to 0.5 M. The TEM images of the nanoparticles are shown in figure 3. The TEM images indicate that size distribution profile of various concentrations of $CaCl_2$ crosslinked polymer nanocarriers with drug. The results showed that particles were composed of well-shaped and nearly spherical shape with a mean diameter of 25 nm. Furthermore, while the concentration of salting out agent increases from 0.05 to 0.5 M, the size of the particles was decreased. It was well correlated with other characterization of nanoparticles. Dynamic light scattering data further demonstrated that the z-potential value of drug-loaded nanoparticles is positive

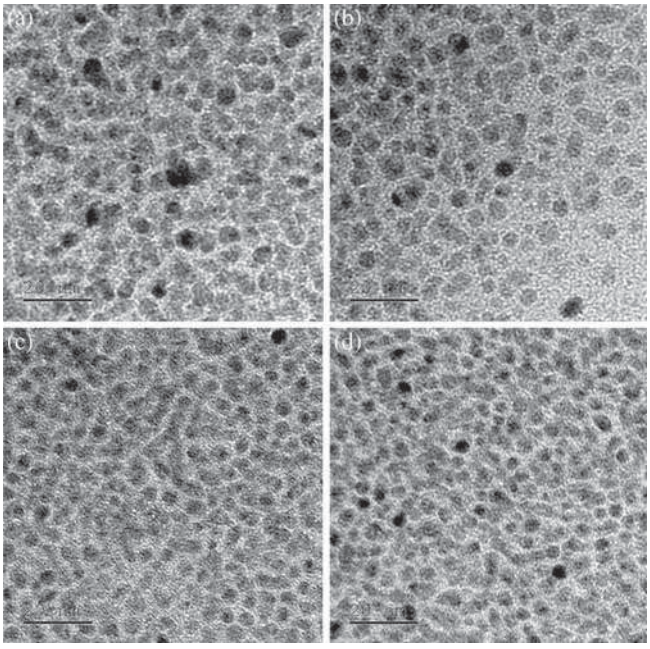


**Figure 3.** TEM images of (**a**) PLA-$CaCl_2$-CDDP-CMC-A, (**b**) PLA-$CaCl_2$-CDDP-CMC-B, (**c**) PLA-$CaCl_2$-CDDP-CMC-C and (**d**) PLA-$CaCl_2$-CDDP-CMC-D nanocomposites.

and drug unloaded nanoparticles is negative. This is due to the binding of CDDP on the polymer matrix. CDDP has two amino groups and so the drug-loaded nanoparticles will attain positive charge when it is in the aqueous solution. At the same time, increase in the concentration of $CaCl_2$ in the synthesis of nanocarriers led to an increase in the z-potential of drug-loaded nanoparticles. The zeta potential values of drug loaded and unloaded nanoparticles are listed in table 1. In the case of without CDDP, composites were decreased, their potential value ranged from –0.19 to –11.04 mV, with the increase in $CaCl_2$ concentration. The magnitude of the zeta potential reflects the surface characteristic of the tested particles. The zeta potential is an important index for the stability of the nanoparticles [32]. Zeta potential value of less than –30 mV or higher than +30 mV assures the stability of nanoparticle suspensions [33]. PLA-$CaCl_2$-CDDP-CMC-D nanocarriers have the Z-potential value of +33.28 mV. This shows that PLA-$CaCl_2$-CDDP-CMC-D nanocarrier has maximum stability than others. Z-potential analysis revealed that concentration of $CaCl_2$ played an important role in determining the charge of drug carriers.

### 3.3 *EE of nanocarriers*

The EE of CDDP loaded on PLA-CMC nanocarriers was studied using UV-visible spectrometer. The EE of CDDP loaded on PLA-CMC nanoparticle with various concentrations of $CaCl_2$ was determined with regular interval time of 30 min and it is shown in figure 4. This spectrum gave the information about EE of nanocarriers in indirect manner. During nanoparticle preparation, every 30 min the nanoparticle supernatant was subjected to evaluation of free drug content. The percentage of absorption in the UV spectrum was directly proportional to the amount of drug present in the supernatant solution. That means unloaded drug gives the absorption spectrum of supernatant solution. On comparison of various concentrations of $CaCl_2$ solution, 0.5 M $CaCl_2$ influenced carriers (PLA-CDDP-CMC-$CaCl_2$-D) that had maximum EE than other compositions, because at 150 min free drug amount was negligible in the supernatant solution of expect. From these observations we report that increase in the concentration of salting out agent increases the EE of the nanocomposites. This is because of the size,

**Table 1.** Zeta potential values of nanocomposites.

| Concentration of $CaCl_2$ (mol $l^{-1}$) | Without drug (mV) | With drug (mV) |
|---|---|---|
| 0.05 | –0.19 | +5.16 |
| 0.20 | –3.92 | +6.52 |
| 0.35 | –8.13 | +17.81 |
| 0.50 | –11.04 | +33.28 |

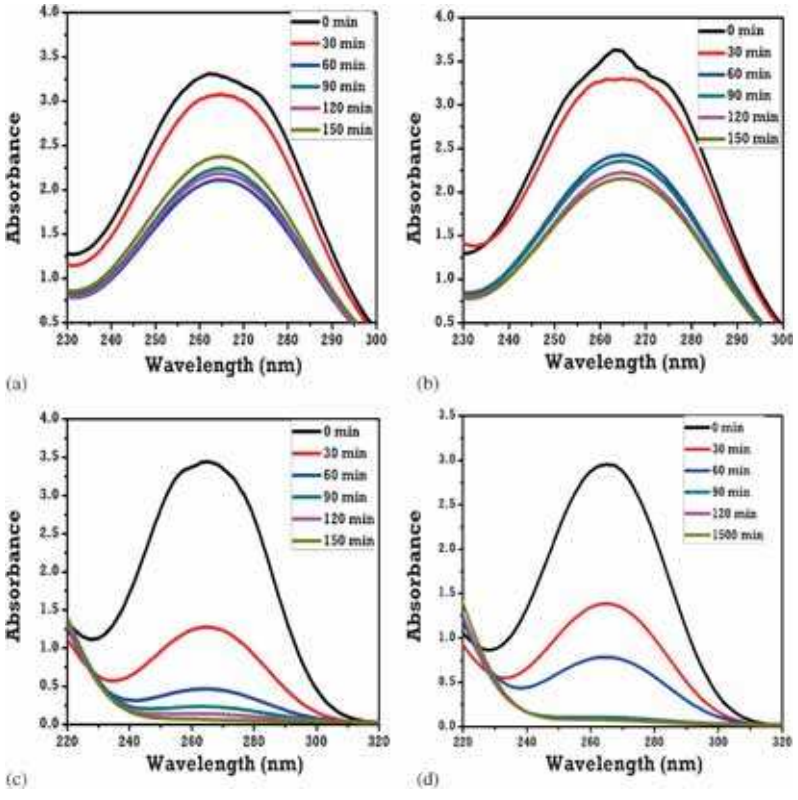


**Figure 4.** Encapsulation efficiency profile of (**a**) PLA-$CaCl_2$-CDDP-CMC-A, (**b**) PLA-$CaCl_2$-CDDP-CMC-B, (**c**) PLA-$CaCl_2$-CDDP-CMC-C and (**d**) PLA-$CaCl_2$-CDDP-CMC-D nanocomposites.

regular arrangement of the particle and stability of the system. It was confirmed by AFM image, because increase in the salting out agent decreased the size of nanocarriers. The comparative EE of the nanoparticles is shown in figure 5.

### 3.4 *In-vitro drug release analysis*

The drug release behaviour of any polymer network depends upon the nature of the polymer, solvent compatibility, degree of crosslinking and the pH environment of the system [33,34]. The drug-releasing behaviour of the formulated nanocarriers (A, B, C, D) was analysed at pH 2.0 and 6.8 by using UV spectroscopy. The *in-vitro* drug-releasing profile of drug-loaded nanocarriers at pH 2.0 is shown in figure 6a–d and i and at pH 6.8 is shown in figure 6e–j. The absorbance in the spectrum is directly proportional to the amount of CDDP released from nanocomposites. On comparison with nanocomposites profile, PLA-CDDP-CMC-$CaCl_2$-D releases more amount of drug than other system. From 0.05 M $CaCl_2$ to 0.5 M $CaCl_2$, the drug-releasing property is increased. It may be the higher amount of drug encapsulated on the system. The concentration of system is dependent on the *in-vitro*-releasing profile. Thus *in-vitro* drug release result is well correlated with results of EE. At pH 2.0, the drug released was comparatively higher than at pH 6.8, because in acidic condition polymer matrix is degraded easily. This shows that designed nanocarriers are pH sensitive. The cancer cells have more acidic nature than normal cells [35]. Because these are our designed carriers, it is easy to deliver out drug from carriers at cancer cells more efficiently than normal cells.

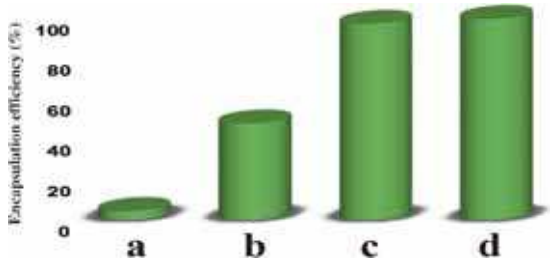


**Figure 5.** Comparative graph of encapsulation efficiency of various carriers.

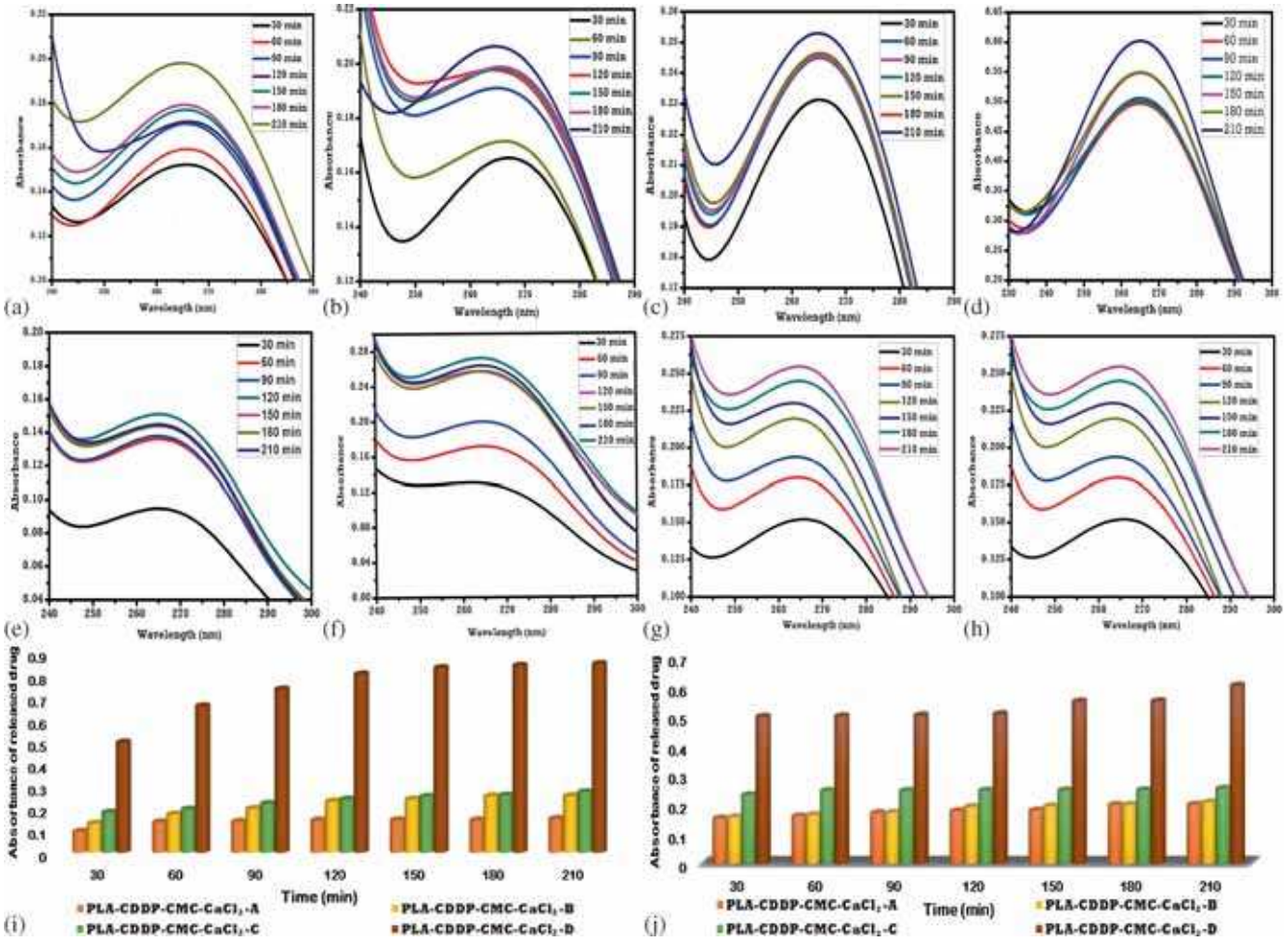


**Figure 6.** (**a**–**d**) *In-vitro* drug release pattern of four carriers at pH 2.0 and (**e**–**h**) at pH 6.8. Comparative drug-releasing pattern at (**i**) pH 2.0 and (**j**) at pH 6.8.

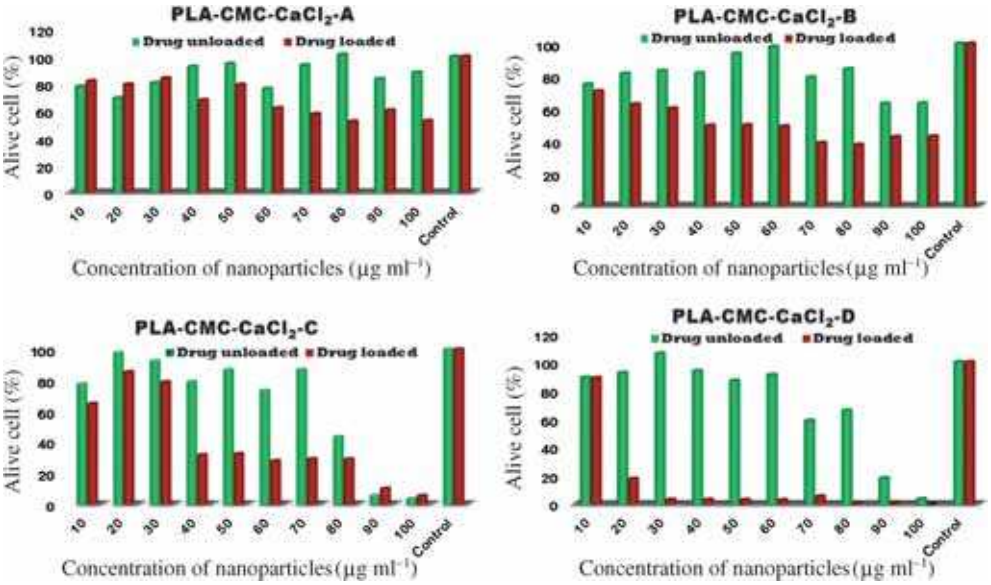


**Figure 7.** Cytotoxicity of nanocomposites against MCF-7 cancer cell line.

### 3.5 *Cytotoxicity of nanoparticles*

The investigation was conducted by dose-dependent cytotoxicity effect with and without nanoparticles against MCF-7 breast cancer cell line. The mean value of obtained triplicate results is shown in figure 7, and all the statistical values are given in supplementary file 1. PLA-$CaCl_2$-CDDP-CMC-A nanocomposite showed $IC_{50}$ value at 70 μg $ml^{-1}$, this is due to its very low EE, whereas PLA-$CaCl_2$-CDDP-CMC-B nanocomposite showed $IC_{50}$ value at 40 μg $ml^{-1}$. $IC_{50}$ value of PLA-$CaCl_2$-CDDP-CMC-C nanocomposite was in between 30 and 40 μg $ml^{-1}$. PLA-$CaCl_2$-CDDP-CMC-D nanoparticle showed $IC_{50}$ value in between 10 and 20 μg $ml^{-1}$. On comparison of four CDDP-loaded formulation, formulation D showed the maximum cytotoxicity in MCF-7 breast cancer cell line than others. The increase in cytotoxicity of nanoparticles with respect to the concentration of salting out agent is due to size and drug encapsulated amount on carriers. PLA-$CaCl_2$-CMC-A and PLA-$CaCl_2$-CMC-B carriers did not expose cytotoxicity effect, but PLA-$CaCl_2$-CMC-C and PLA-$CaCl_2$-CMC-D carriers showed slight cytotoxicity at 80 μg $ml^{-1}$ concentration to the cancer cells. This is may be due to high concentration of $CaCl_2$ present in the carriers. The results revealed that all unloaded PLA-CMC graft copolymer composites were practically non-toxic up to a tested concentration, indicating that PLA-CMC particles have excellent biocompatibility. The low cytotoxicity and intrinsic biodegradability of PLA-CMC carriers render them particularly interesting for further *in-vivo* applications.

## 4. Conclusion

Cisplatin-loaded CMC crosslinked PLA nanoparticle was successfully formulated with controlled size using various concentrations of $CaCl_2$ as salting out agent. The drug-conjugated carriers were confirmed by FT-IR spectroscopy analysis. The size of the synthesized carriers was determined using AFM study, and the surface morphology of synthesized carriers was confirmed by TEM measurement. Zeta potential results show that nanoparticles have apparently very high stability and opposite charge of the cell membrane. The size of the composites was controlled by the concentration of salting out agent. The EE of the nanoparticle was increased linearly with the increase in concentration of salting out agent. Cytotoxicity study shows that carrier has good biocompatibility and drug-loaded nanoparticles exhibit considerable cytotoxicity against MCF-7 breast cancer cell line. The nanocarriers derived from 0.5 M $CaCl_2$ have the optimum properties than the others and they delivered anti-cancer drug potentially to targeted sites.

## Acknowledgements

M Rajan is grateful to the University Grants Commission (UGC), Government of India, for providing financial assistance under the scheme of 'UGC-BSR Research Start-Up Grants' (Ref: No.F.30-21/20014 (BSR). Rajan also thanks the University Grants Commission, New Delhi, for funds under the PURSE, UPE program. We would like to extend our sincere appreciation to the Deanship of Scientific Research at King Saud University for its funding of this research through the Research Group project No. RG-1435-065.

## Conflict of interest

We report no conflicts of interest. We alone are responsible for the content and writing of the paper.

## Electronic Supplementary Material

Supplementary Material pertaining to this article is available on the Bulletin of Materials Science website (www.ias.ac.in/matersci).

## References


[1] Bhowmik D, Chiranjib, Margret Chandira R, Tripathi K K and Sampath Kumar K P 2010 *Int. J. PharmTech. Res.* **2** 2143

[2] Gupta A S 2011 *Nanomed. Nanotechnol. Biol. Med.* **7** 763

[3] Shapira A, Livney Y D, Broxterman J H and Assaraf Y G 2011 *Drug Resist. Updat.* **14** 150

[4] Kranti P M, Praful B D, Prashant B M, Naseer Maliyakkal M, Ranjith Kumar A, Sreenivasa Reddy M and Udupa N 2014 *Bull. Mater. Sci.* **37** 945

[5] Thambi T, Deepagan V G, Yoon H Y, Han H S, Kim S H, Son S, Jo D G, Ahn C H, Suh Y D, Kim K, Kwon I C, Lee D S and Park J H 2014 *Biomaterials* **35** 1735

[6] Panyam J and Labhasetwar V 2003 *Adv. Drug Deliv. Rev.* **55** 329

[7] Yoo J W, Doshi N and Mitragotri S 2011 *Adv. Drug Deliv. Rev.* **63** 1247

[8] Lepeltier E, Bourgaux C and Couvreur P 2014 *Adv. Drug Deliv. Rev.* **71** 86

[9] Iversena T G, Skotlanda T and Sandvig K 2011 *Nano Today* **6** 176

[10] Astete C E and Sabliov C M 2006 *J. Biomater. Sci. Polym. Ed.* **17** 247

[11] Ranjith K A, Gopal V S, Aravind K G, Praful B D, Karthik A, Naseer M, Sreenivasa R M and Udupa N 2012 *Bull. Mater. Sci.* **35** 319

[12] Pal S L, Jana P, Manna P K, Mohanta G P and Manavalan R 2011 *J. App. Pharm. Sci.* **6** 228

[13] Soppimath K S, Aminabhavi T M, Kulkarni A R and Rudzinski W E 2001 *J. Control Release* **70** 1

[14] Hans M L and Lowman A M 2002 *Curr. Opin. Solid State Mater. Sci.* **6** 319

[15] Barichello J M, Morishita M, Takayama K and Nagai T 1999 *Drug Dev. Ind. Pharm.* **25** 471

[16] Quintanar-Guerrero D, Allemann E, Fessi H and Doelker E 1998 *Drug Dev. Ind. Pharm.* **24** 1113

[17] Bankar S K, Chaudhari A V, Mahale N B and Chaudhari S R 2014 *J. Adv. Drug Deliv.* **1** 82

[18] Ibrahim H, Bindschaedler C, Doelker E, Buri P and Gurny R 1992 *Int. J. Pharm.* **87** 239

[19] LeHoux J G and Dupuis G 2007 *Carbohydr. Polym.* **68** 295

[20] Fischer B, Heffeter P, Kryeziu K, Gille L, Meier S M, Berger W, Kowol C R and Keppler B K 2014 *Dalton Trans.* **43** 1096

[21] El-Hag Ali A, Abd El-Rehim A, Kamal H, Hegazy D and El-Sayed A 2008 *J. Macromol. Sci. Pure Appl. Chem.* **45** 628

[22] Galindo-Rodriguez S, Allemann E, Fessi H and Doelker E 2004 *Pharm. Res.* **21** 1428

[23] Tabatabaei Rezaei S J, Nabid M R, Niknejad H and Entezami A A 2012 *Polymer* **53** 3485

[24] Nagavarma B V N, Hemant K S Yadav, Ayaz A, Vasudha L S and Shivakumar H G 2012 *Asian J. Pharm. Clin. Res.* **5** 16

[25] Basavaraja C, Kim J K and Huh D S 2013 *Mater. Sci. Eng. B* **178** 167

[26] Biswal D R and Singh R P 2004 *Carbohydr. Polym.* **57** 379

[27] Habibi N 2014 *Spectrochim. Acta Part A* **131** 55

[28] Bajpai A K and Sweta L 2013 *Bull. Mater. Sci.* **36** 15

[29] Wokadala O C, Emmambux N M and Ray S S 2014 *Carbohydr. Polym.* **112** 216

[30] Wang Y, Zhou J, Qiu L, Wang X, Chen L, Liu T and Di W 2014 *Biomaterials* **35** 4297

[31] Lei D, Liu J, Ye F, Chen F and Zhao G 2014 *Food Hydrocolloids* **41** 250

[32] Rajan M, Raj V, Al-Arfaj A A and Murugan A M 2013 *Int. J. Pharm.* **453** 514

[33] Muzzarell R A A, Tanfani F, Mariotti S and Emanuelli M 1982 *Carbohydr. Polym.* **2** 145

[34] Kumari K and Kundu P P 2008 *Bull. Mater. Sci.* **31** 159

[35] Du J Z, Mao C Q, Yuan Y Y, Yang X Z and Wang J 2014 *Biotechnol. Adv.* **32** 789